Design Optimization of Uncoupled Six-core Fibers in Standard Cladding Diameter Using Artificial Intelligence

Xun Mu, Filipe M. Ferreira, Alessandro Ottino, Georgios Zervas

Optical Network Group, University College London, London, WC1E 7JE,UK

xun.mu.17@ucl.ac.uk

Abstract: We report on ultra-wide-band and long-haul compatible 125μm six-core trench-assisted fiber designs. The AI-optimization process considers crosstalk, effective area, and bandwidth. We show that homogeneous cores can lead to low complexity yet high capacity fiber.

OCIS codes: (060.2280) Fiber design and fabrication; (060.2310) Fiber optics.

1. Introduction

Multi-core fibers (MCFs) have revealed their ability to improve the network performance, to augment the front panel density while delivering increased energy and cost efficiency [1]. In previous works, MCF optimization involves only a subset of the parameters that describe the refractive-index profile. However, the optimal solution requires all the parameters to be explored. Targeting such a complex problem with a brute force method would be time-consuming and impractical, especially for heterogeneous MCFs (Hete-MCFs). Instead, we propose using artificial intelligence to optimize the design of Hete-MCFs over all parameters. Particle swarm optimization (PSO) [2, 3] is chosen as it can significantly reduce the number of permutations evaluated (from $\sim 10^{15}$ to $\sim 10^{6}$). Moreover, the computation of coating loss is sped up (from $\sim$ 100s to $\sim 14\mu$s) using a statistical classifier based on neural networks. In this paper, we successfully designed three six-core MCFs covering different bandwidths while keeping crosstalk (XT) ≈ -63 dB/km and achieving an effective mode area (A_{eff}) comparable to that of conventional single-mode fiber. As part of the overall design process the signal-to-noise ratio (SNR) and capacity of the fibers are also estimated.

2. Crosstalk Calculation and Optimization

In this work, we choose the single-ring structure to avoid the cut-off wavelength elongation and XT degradation of the central core. The 6-core symmetrical fiber structure has two types of cores to reduce XT and bending sensitivity through the phase mismatching between neighbouring core pairs. The core pitch is set at 32.5 μm. This structure allows to simplify the MCF design problem by focusing on neighbouring core-pair optimization. Fig.1. shows the layout diagram and the core index profile of the trench-assisted Hete-MCF considered. The outer cladding thickness (OCT) is assumed as 30 μm. The excess loss caused by coating is kept lower than 0.001 dB/km [4]. The coating loss is defined as the outermost core's bending loss of LP01 at 1625 nm with bending radius as 140 mm and coating index as 1.475. To speed up the coating loss computation we used a statistical classifier to check whether or not the coating loss of the core is higher than 0.001 dB/km — using the finite difference eigenmode (FDE) solver in Lumerical [19] would take more than 120s. The classifier was implemented using a 5-layer fully-connected neural network trained with 7000 cases generated with the FDE solver — we used the relu activation function [5] and the Adam optimizer [6] and demonstrated a 99.98% accuracy. Classifier inference time is 14 μs on Nvidia V100 GPU for single calculation (10^6–times faster than FDE).

We assume that the core is doped with germanium, the trench is doped with fluorine [7] and that the inner cladding and the outer cladding are both assumed to be pure silica. Table 1 shows the index-profile parameters considered. Note that only discrete values are considered to simplify the fabrication of the optimized MCFs. To explore all the parameters combinations in Table 1, there would be $(21\times51\times51\times31\times36)^2 = 3.7\times10^{15}$ permutations. However, with PSO, the optimized solution is explored intelligently after no more than 1.76×10^6 permutations (10^9 fewer permutations).

In this paper, the mean of the IC-XT over all the cores is considered as the optimization indicator. The mean IC-XT for Hete-MCFs is given by [8]:

$$IC\text{-}XT_p = \left(n - \sum_{i=1}^{n} e^{-(n+1)h_{pq}L}\right) \Big/ \left(1 + \sum_{i=1}^{n} e^{-(n+1)h_{pq}L}\right) \tag{1}$$

where p is the target core, q is any of its n neighbors, h_{pq} is the average power coupling coefficient (PCC) [18] between p and q, and L is the fiber length. This XT model has been verified against experimental values for fabricated MCFs [13].

In PSO, each particle is a potential solution to the problem, denoted as X_p. In this MCF design, each particle is a set of MCF structure parameters: 10 variables in total with 5 parameters as in Table 1 for each of the two core types. For each particle, a fitness value is calculated using the objective function, which includes the penalty for not satisfying a design constraint and the XT. In this way, a smaller fitness value implies a better particle/design. The optimization direction is described by the velocity V_p. During the optimization process, each particle makes appropriate adjustment of the optimization direction and particle itself at each iteration as Eq. (2) [10] . The decision is influenced by the

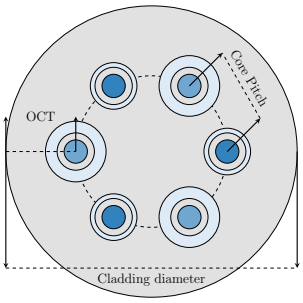

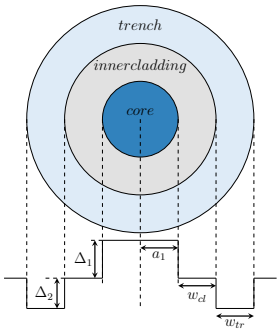

Parameters	Range	Step	Choices
a_1 [μm]	$4 \sim 6$	0.1	21
w_{cl} [μm]	$2.5 \sim 7.5$	0.1	51
w_{tr} [μm]	$2.5 \sim 7.5$	0.1	51
Δ_1	$0.3\% \sim 0.6\%$	0.01%	31
Δ_2	-0.7% $\sim$ -0.35%	0.01%	36

Fig. 1. (a) Trench-assisted Hete-MCF layout; (b) TA core index profile diagram; Table 1 Index parameters per core.

best parameter set with the smallest fitness value that the particle itself found so far (*pbest*) and that decided by the global group communication (*gbest*). With the particles keeping learning to reduce the fitness value, when the particles converge, the minimal fitness value and its corresponding parameter set is found.

$$X_p^{'} = X_p + V_p^{'} = X_p + [\omega V_p + c_1 * rand() * (pbest - X_p) + c_2 * rand() * (gbest - X_p)] \quad (2)$$

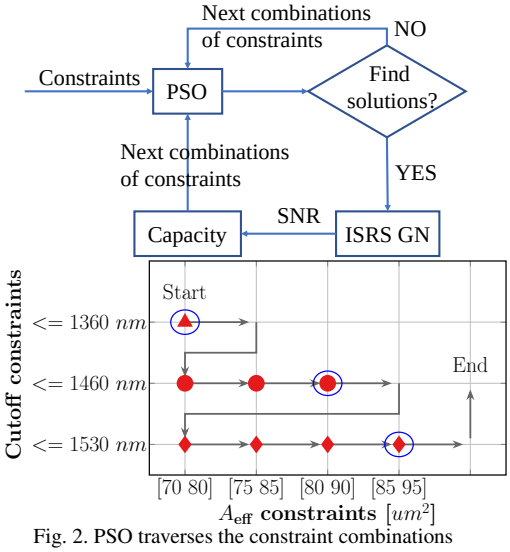

Fig. 2. PSO traverses the constraint combinations

In this paper, five constraints are included on MCF design in total. Besides that of the coating loss, there are two more conducted for all the MCFs designs: a) the distance between adjacent trench edges must be larger than 2 μm [9] to prevent the cores overlapping with each other; b) the chromatic dispersion (D) at 1550 nm is constrained between 16 and 25 ps/km/nm. The other two are the cut-off wavelength and A_{eff} constraints. For the latter two constraints, PSO goes through their combinations to explore the highest A_{eff} constraint which can be satisfied for each cut-off constraint case, as illustrated in Fig. 2. It starts from the widest bandwidth — cut-off wavelength $\leq$ 1360 nm — and the smallest A_{eff} constraint — $A_{\text{eff}} \in$ [70 80] μm^2. The PSO is ran ten times for each constraint combination to test its reliability. Before moving to the next constraint combination, if the PSO finds solutions satisfying all the constraints, the MCF parameter set is passed to the inter-channel stimulated Raman scattering Gaussian Noise (ISRS GN) model [11] that calculates the SNR and respective capacity. The next constraint combination is preferentially obtained by moving forward on the A_{eff} constraint, only if the PSO cannot find proper solution, the constraint combination will change to narrower bandwidth. Section 3 focus only on the MCF solutions obtained for the highest A_{eff} constraint, for each of the cut-off, indicated in Fig.2. by blue circles.

Non-overlapping and coating loss constraints are checked at the beginning of the objective function. If both constraints are satisfied, the fitness value is equal to $XT + penalty_D + penalty_{A_{\text{eff}}} + penalty_{\text{cut-off}}$ where the penalty for each characteristic is the difference between the calculated value and the average of the boundaries, for example, for A_{eff} this is: $penalty_{A_{\text{eff}}} = (\sum_1^2 |A_{\text{eff}}^i - 75|)^2$ for two core types if $A_{\text{eff}} \notin$ [70 80] μm^2, otherwise $penalty_{A_{\text{eff}}} = 0$. Instead, if one or both of these conditions are not satisfied the permutation is not fully evaluated and a large penalty, of the order of 10^7, is given to the fitness value. In this way, we further reduce the problem space and computation time.

3. Results and Discussion

For each of these constraints combinations highlighted in Fig.2., the PSO is ran 10-times obtaining in all cases solutions satisfying all the constraints. All runs converged to similar XT [dB/km] and A_{eff} [μm^2] values, standard deviation < 0.34 and < 0.46, respectively. The lowest XT obtained for these three cases are -64 dB/km, -63.3 dB/km and -63 dB/km, respectively, at 1550 nm for a bending radius of 140 mm [4]. Notably, despite allowing for the flexibility of an heterogeneous core arrangement, in all three MCF design cases both core types have very similar parameters. The *gbest*s obtained in the ten PSO runs are shown in Fig.3.(a) for cut-off $\leq$ 1360 nm as an example. Consequently, these quasi-homogeneous cores have a very small n_{eff} difference ($< 7 \times 10^{-6}$) and their PCC was found to increase linearly with the bending radius (at least up to 500 mm). Fig.3.(b) compares the XT and relative core multiplicity factor (RCMF) [17] of the solutions found here with those of other MCFs with standard cladding diameter found in the literature. All the solutions in our work matched the lowest XT achieved previously but with up to 45.2% higher RCMF.

The SNR is calculated using the ISRS GN model considering the XT as an extra noise source [12]. The calculation

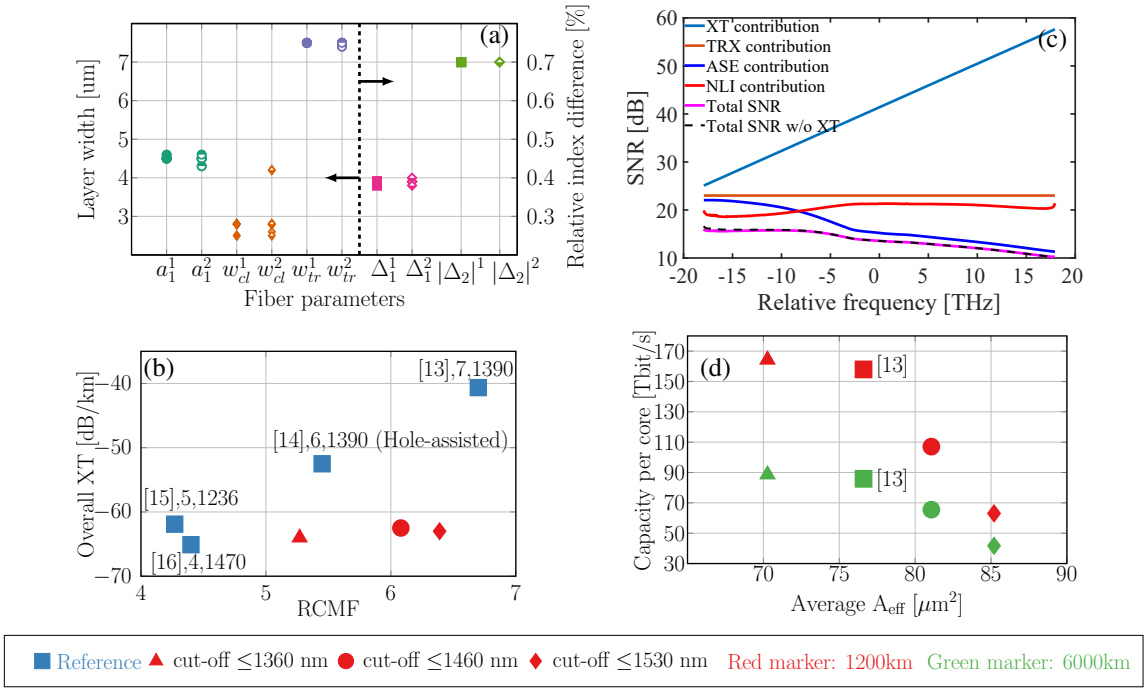

Fig. 3. (a) Parameters in *gbest* of ten runs obtained in cut-off $\leq$ 1360 nm case (the superscript indicates which core the parameter belongs to); (b) Comparison between our work with fabricated 125 μm cladding diameter fiber with silica cladding ([ref],core number,cut-off); (c) SNR of the MCF core obtaining with cut-off $\leq$ 1360 nm and $A_{eff} \in$ [70 80] μm^2 for 1200 km transmission; (d) Capacity per core of our work for two transmission length compared to that of [13].

assumes Gaussian modulation, uniform launch power -2 dBm/channel, bandwidth 50 GHz per channel, 60 km per span and 5 dB noise figure optical amplification. Total SNR and a breakout of its various contributions for 1200 km are illustrated in Fig.3.(c). The XT contribution has negligible influence on the total SNR for the fibers in this paper. Fig.3.(d) shows the capacity per core for the optimum fiber designs — calculated as the sum of the channel capacity over the optical bands within the design cut-off constraint. The six-core fiber optimized here for the shortest cut-off wavelength constraint covers E+S+C+L-bands, capable of carrying 164.2 Tbit/s capacity per core which is higher than that in [13]. The total capacity of this MCF is $\approx$0.98 Pbit/s. As expected from Shannon's law, the capacity per core mainly determined by the cut-off wavelength despite an increase in the A_{eff}. However, A_{eff} influence can be seen when the total fiber length increases from 1200 km to 6000 km, the capacity per core of the widest bandwidth and smallest A_{eff} drops by 45.8% to 88.6 Tbit/s, while that of the largest A_{eff} but only covering C+L band just decreases by 33.8%.

4. Conclusion

We designed three 6-core fibers supporting multiple wavelength bands with ultra-low XT (-63 dB/km) while considering fabrication limits and optical property constraints. The fiber designs here matched the best XT performance achieved in literature but with up to 45.2% higher RCMF. In the design process we used PSO reducing the search space by $\sim 10^9$ permutations, and statistical classifier that evaluates the coating loss condition $\sim 10^6\times$ faster than a FDE solver. ISRS GN model was used to calculate the SNR across 40 THz of bandwidth. One fiber is capable of 164.2 Tbit/s/core or nearly 1 Pbit/s over E+S+C+L-bands after 1200 km. The design process converged to a solution of homogeneous cores that reduces fabrication complexity. The methods proposed here offer promising tools for the design of future fibers.

The work is supported by EPSRC EP/L015455/1, OptoCloud EP/T026081, TRANSNET EP/R035342 & UKRI FLF MR/T041218.

References

[1] H.Yuan *et al*. JOCN, 10, 272-288 (2018)
[2] J.Kennedy *et al*. *Encyclopedia of machine learning*, 760–766 (2010)
[3] J.Mata *et al*. OSN, 28, 43-57 (2018)
[4] T.Hayashi *et al*. JLT, 30, 583-589 (2011)
[5] Nair *et al*. ICML, 807–814 (2010)
[6] Diederik P. Kingma *et al*. arXiv (2017)
[7] W. Hermann *et al*. *Materials Research Bulletin*, 1083-1097 (1989)
[8] G.M.Saridis *et al*. *IEEE Communications Surveys & Tutorials*, 17, 2136–2156 (2015)
[9] J. Tu *et al*. *Opt.Express*, 20, 15157-15170 (2012)
[10] A.Carlisle *et al*. *Proc. of the workshop on PSO* (2001)
[11] D. Semrau *et al*. ECOC, W.1.D. (2019)
[12] R. S. Luís *et al*. JSTQE, 26, 1-9 (2020)
[13] K. Takenaga, *et al*. OFC, OWJ4 (2011)
[14] T. Sakamoto *et al*. ECOC, Mo.3.A.3 (2013)
[15] T. Gonda *et al*. ECOC, W.2.B.1 (2016)
[16] Y. Sagae *et al*. OECC, TuC3-4 (2019)
[17] S. Matsuo *et al*. *Opt.Letters*, 36, 4626–4628 (2011)
[18] M. Koshiba *et al*. *Photon.Journal*, 4,1987–1995 (2012)
[19] Lumerical Inc. https://www.lumerical.com/products/